2007 IEEE International Conference on
Robotics and Automation
Roma, Italy, 10-14 April 2007



# Virtual Fixture Control for Compliant Human-Machine Interfaces

Panadda Marayong, Hye Sun Na, and Allison M. Okamura

*Abstract*— **In human-machine collaborative systems, robot joint compliance and human-input dynamics lead to involuntary tool motion into undesired regions. To correct this, a set of methods, called Dynamically-Defined Virtual Fixtures, was previously proposed to create a movable virtual fixture that stops the user at a safe distance outside the forbidden region. In this work, a new method, called the Force-Based Method, was added. A vision system was introduced for real-time tool tracking. Additionally, we implemented a closed-loop controller with the virtual fixtures that allows the user to reach, but not enter, the forbidden region. Two user experiments were conducted on a 1-DOF testbed to evaluate the virtual fixture methods. The first experiment showed the effectiveness of the virtual fixtures in preventing the penetration. However, the absence of haptic feedback in the closed-loop implementation resulted in boundary penetration. In the second experiment, visual feedback was used to compensate for the lack of haptic feedback. User cognitive load was added as an inhibiting factor in a human-machine cooperative setting. The experiment showed a significant reduction in penetration with visual feedback, while the addition of cognitive load did not significantly increase the penetration.**

## I. Introduction

Human-machine cooperative systems offer an ideal setting in which the precision and repeatability of a robot are combined with the intelligence and experience of a human operator. Software-generated virtual fixtures can be added to these systems to guide a tool along desired paths in the workspace (Guidance virtual fixtures) or to prevent the tool from entering undesired regions (Forbidden-Region virtual fixtures) [1], [2], [10], [12], [13], [14]. During cooperative manipulation with an admittance-controlled system, the human operator actively exerts force on the tool to generate robot motion. The JHU Steady-Hand Robot [15] shown in Figure 1(a) is an example of such a system. Despite its high rigidity and non-backdrivability, previous experiments show that even small joint and link compliance visibly degrade virtual fixture performance [9]. Unmodeled deviations in the mapping from robot joint space to the environment/task space cause the virtual fixture location to be incorrectly defined. The operator's hand dynamics and cognitive delay that occur at the time of virtual fixture contact result in additional tool motion. With the robot compliance, this motion causes the tool to move in an undesired direction/region.

Our work focuses on the evaluation of control methods developed for implementing Forbidden-Region virtual fixtures on a system with joint compliance. With Forbidden-Region virtual fixtures, the tool is prevented from entering into an undesired region while giving the operator total freedom to manipulate the tool outside of the region. In [11], we presented a set of methods, called *Dynamically-Defined Virtual Fixtures*, to create a movable virtual fixture that stopped the tool at a safe location in front of the forbidden region. The two methods proposed were the Velocity-Based and Hand-Dynamic Methods. Specifically, the methods predict the amount of potential overshoot due to the system dynamics and use the information to define the new virtual fixture position. In the Hand-Dynamic Method, the user's hand dynamics were included in the model. The two methods were implemented in an open-loop fashion, where the robot was stopped once the algorithm determined the possibility of an overshoot. The experimental results in [11] showed that the methods effectively prevented forbidden-region penetration; however, the tool was stopped at a conservative distance outside the region. This deviation may not be desirable in applications that require the tool to be manipulated closer to or on the surface of the forbidden region. In this work, we extend the virtual fixture methods to include a closed-loop control that allows the user to reach the forbidden region following an overdamped trajectory. In addition, a

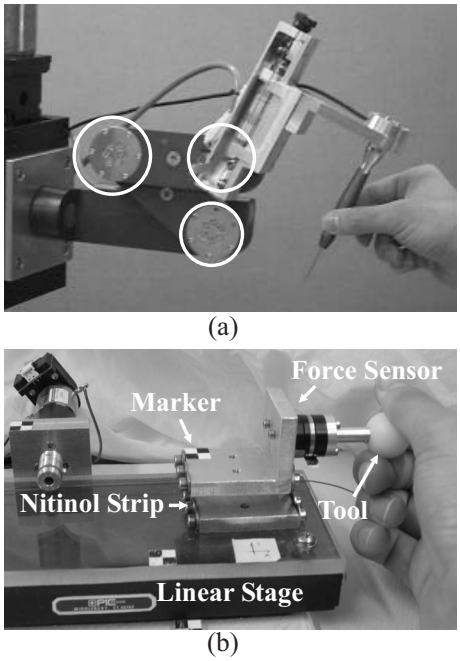


(a)

(b)

Fig. 1. (a) The Steady-Hand Robot [15] with locations of joint compliance circled. (b) The 1-DOF testbed with four Nitinol strips connecting the tool and the stage to simulate joint compliance.

This work was supported by NSF Grants ITR-0205318 and EEC-9731748

P. Marayong and A. Okamura are with the Engineering Research Center for Computer-Integrated Surgical Systems and Technology, Johns Hopkins University, Baltimore, MD 21218, USA pmarayong@jhu.edu, aokamura@jhu.edu

H. Na is with the Department of Biomedical Engineering, University of Texas, Austin, TX 78712, USA hyesunna@mail.utexas.edu

TABLE I
LIST OF SYSTEM VARIABLES

| Variable | Description |
|---|---|
| $x_t, \dot{x}_t$ | Tool position and velocity |
| $x_s, \dot{x}_s$ | Stage position and velocity |
| $x_h, \dot{x}_h$ | Virtual hand position and velocity |
| $x_f$ | Forbidden-region boundary position |
| $x_w$ | Dynamically-defined virtual fixture position |
| $d$ | Safety margin to be determined |
| $m_t, k_t$ | Tool mass and stiffness coefficient |
| $m_h, b_h, k_h$ | Hand mass, damping and stiffness coefficients |
| $f_a$ | Applied force measured by force sensor |

new Dynamically-Defined Virtual Fixture method, called the Force-Based Method, is introduced. This method considers the user's input force measured from the force sensor without considering the hand dynamics in the model.

This paper provides the descriptions of the Dynamically-Defined Virtual Fixtures for open- and closed-loop control. Two user experiments were conducted to evaluate the performance of each method using the same 1-DOF admittance-controlled testbed from [11], shown in Figure 1(b). In this work, a vision system was added to obtain the tool and stage position through real-time visual tracking.

## II. DYNAMICALLY-DEFINED VIRTUAL FIXTURES

Robots of the admittance type are non-backdrivable with velocity-source actuators. The robot motion is governed by

$$\dot{\vec{x}} = C\vec{f}, \tag{1}$$

where $\dot{\vec{x}}$ and $\vec{f}$ are vectors representing the output velocity and the force/torque input, respectively. $C$ is the admittance gain matrix. Forbidden-Region virtual fixtures are created by setting the element of $C$ that corresponds to the motion in the undesired direction (region) to zero. For a 1-DOF system, this reduces to simply preventing the tool tip from passing a fixed limit.

Table I describes the system variables used in the remainder of the paper. In a 1-DOF system, these variables are scalar quantities. Let $x_w = x_f + d$ denote the dynamic virtual wall position for a desired safety margin, $d$. The following sections describe the Dynamically-Defined Virtual Fixture methods for choosing $d$ to ensure that $x_t < x_f$, despite the effects of robot compliance and hand dynamics. The methods can be extended to a system with higher degrees of freedom, with the caveat that the following methods assumed a linear dynamical system.

### A. Velocity-Based Method

The Velocity-Based Method provides an ad hoc solution to estimate the amount of overshoot that will occur if the operator continues moving with the same instantaneous velocity. The future tool position is predicted from the current tool position and velocity. The condition applied by the method to determine the dynamic virtual wall position, $x_w$, is

$$x_w = \begin{cases} x_t & \text{if} \quad x_t + \Delta t \dot{x}_t > x_f \\ x_f & \text{otherwise} \end{cases}, \tag{2}$$

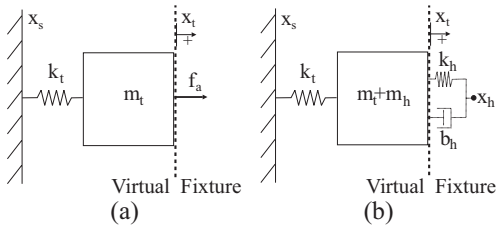


Fig. 2. (a) System model with force input from the force sensor. (b) Hand and system model used by the Hand-Dynamic Method.

where $\Delta t$ is the time step used to calculate a future tool position. In our implementation, $\Delta t = 120$msec, since this represents the time required for a human to voluntarily respond to a tactile stimulus with a motor command [4]. During this time, the applied force is assumed to be constant.

### B. Force-Based Method

In an admittance-controlled system, the user's force input is measured by a force sensor to command the robot motion. Hence, the equation of motion describing the tool position with joint compliance can be determined based on the system schematic shown in Figure 2(a) as

$$m_t \ddot{x}_t + k_t(x_t - x_s) = f_a. \tag{3}$$

The maximum tool position, $x_{t,\max}$, can be determined in closed-form as

$$x_{t,\max} = \left(\sqrt{a^2 + b^2}\right) + x_{s,o} + \frac{f_a}{k_t}, \tag{4}$$

$$\text{where} \quad a = x_{t,o} - x_{s,o} + \frac{f_a}{k_t}$$

$$b = \left(\sqrt{\frac{m_t}{k_t}}\right)\dot{x}_{t,o}.$$

The subscript $o$ indicates the initial condition. At every time step, we assume a new reference ($x_{s,o} = x_{t,o} = 0$) to determine $x_{t,\max}$. The method then computes the virtual fixture position using the following condition:

$$x_w = \begin{cases} x_t & \text{if} \quad x_t + x_{t,\max} > x_f \\ x_f & \text{otherwise} \end{cases} \tag{5}$$

### C. Hand-Dynamic Method

The Hand-Dynamic Method includes the system model used in the Force-Based Method, but is modified by incorporating a hand model to capture the instantaneous involuntary hand motion. In our analysis, the hand motion is described by the equilibrium-point control model shown to be valid for a slow limb motion in [3]. The requisite force exerted by the limb is proportional to the limb stiffness ($k_h$) and the instantaneous difference between the virtual equilibrium position ($x_h$) and the actual limb position ($x_{\text{actual}}$):

$$f_a = k_h(x_h - x_{\text{actual}}). \tag{6}$$

In applications such as microsurgery, most of the motion occurs from the hand and the wrist, while the forearm and the upper arm remain stationary. Hence, only the hand and

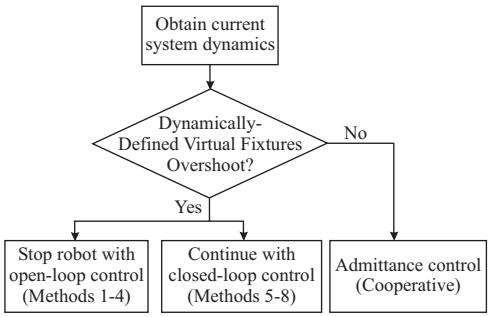


Fig. 3. Flowchart shows the implementation of the Dynamically-Defined Virtual Fixture methods and the closed-loop controller.

wrist dynamics are considered and modeled with a mass-spring-damper model, which has been shown accurate for the modeling of the human upper-extremity joints [5], [7], [16]. Figure 2(b) represents the interaction between the hand and the robot at the virtual fixture. The equation of motion describing the tool position is

$$m_{th}\ddot{x}_t = k_t(x_s - x_t) + k_h(x_h - x_t) + b_h(\dot{x}_h - \dot{x}_t), \quad (7)$$

where $m_{th}$ is the mass of the tool plus the hand. Since the hand is assumed to maintain contact with the tool at all times, the tool and hand are at the same position, $x_t$. Between each time step, the applied force is assumed to be constant. Hence, the virtual hand position, $x_h$, can be estimated from (6). The virtual hand velocity, $\dot{x}_h$, is assumed to be zero. Note here that the force can be measured at every time step with the force sensor. Substituting (6) into (7), the maximum tool position at every time step, $x_{t,\max}$, can be calculated in closed-form as

$$x_{t,\max} = \sqrt{a^2 + b^2}\ \exp\left(\frac{-b_h t_{\max}}{2m_{th}}\right) + c \quad (8)$$

$$\text{where} \quad a = \frac{k_t(x_{t,o} - x_{s,o}) - f_a}{(k_t + k_h)}$$

$$b = \frac{2\dot{x}_{t,o}m_{th} + b_h a}{\sqrt{4m_{th}(k_t + k_h) - b_h^2}}$$

$$c = \frac{k_t x_{s,o} + k_h x_{t,o} + f_{a,i}}{k_h + k_t}$$

The subscript $o$ denotes initial conditions. At every time step, we assume a new reference ($x_{s,o} = x_{t,o} = 0$) to determine $x_{t,\max}$. The method then predicts the maximum tool position if the operator continues moving with the current applied force. The algorithm then computes the position of the virtual fixture using the condition described in (5). The values of the hand dynamic parameters were obtained from [11].

## III. Closed-Loop Controller

As mentioned earlier, it is desirable to manipulate the tool closer to or on the forbidden region. This is not possible with the Dynamically-Defined Virtual Fixtures when the methods are applied in an open-loop fashion. Hence, a closed-loop controller is proposed to allow the tool to approach the forbidden-region without penetrating past its boundary.

With the presence of joint compliance under active manipulation, human input acts as a disturbance to the system.

TABLE II

Dynamically-Defined Virtual Fixture methods numbered by their respective open-loop and closed-loop implementation.

| Methods | Method Number | |
|---|---|---|
| | Open loop | Closed loop |
| Velocity-Based | 1 | 5 |
| Force-Based | 2 | 6 |
| Hand-Dynamic without Hand Damping | 3 | 7 |
| Hand-Dynamic with Hand Damping | 4 | 8 |

The task of approaching the forbidden region becomes the problem of reference tracking with disturbance rejection on the tool position. To prevent the overshoot, the controller must correct for the transient response of the disturbance force. The closed-loop controller proposed in this work aims to determine the desired robot velocity that will result in an overdamped trajectory of the tool toward the forbidden region to prevent boundary penetration. The disturbance is accounted for by feeding forward the instantaneous system dynamics in the controller.

Based on the admittance control law in (1), the force generated on the tool from the system can be modelled by the inverse relationship, $\vec{f} = C^{-1}\dot{\vec{x}}$. Incorporating this relationship on the 1-DOF system described in Figure 2(a), we obtain

$$m_t\ddot{x}_t + k_t(x_t - x_s) = f_s + f_a \quad (9)$$

$$\text{where} \quad f_s = \frac{\dot{x}_s}{c_{\text{ad}}} \quad (10)$$

where $\dot{x}_s$ is the desired stage velocity to be determined. $f_s$ is the force generated by the stage and $c_{\text{ad}}$ is the stage admittance gain. Assuming a known constant position of the forbidden-region boundary, $x_f$, and setting the stage force as

$$f_s = -f_a - k_1\dot{x}_t + k_2(x_f - x_t) + k_t(x_t - x_s), \quad (11)$$

with a change of coordinate, we obtain the system model as

$$m_t\ddot{e} + k_1\dot{e} + k_2 e = 0, \quad (12)$$

$$\text{where} \quad e = x_f - x_t.$$

The system described in (12) is controllable. The gains $k_1$ and $k_2$ can be selected so that the system is asymptotically stable and the tool position, $x_t$, reaches the target reference, $x_f$, in an overdamped fashion. Hence, by applying (10) and (11), the desired stage velocity, $\dot{x}_s$, can be calculated. The gains $k_1$, $k_2$, and $c_{\text{ad}}$ are determined experimentally.

With the closed-loop controller active, the operator loses the freedom to control the motion of the base stage. This characteristic may be undesirable. To account for this, the closed-loop controller is activated only when the Dynamically-Defined Virtual Fixture methods discussed in the previous sections determine the possibility of overshoot. The flowchart shown in Figure 3 outlines the system implementation. The four methods used to predict the overshoot include: Velocity-Based, Force-Based, Hand-Dynamic without hand damping, and Hand-Dynamic with hand damping. These open-loop methods will be referred to as Methods 1 through 4, respectively. Accordingly, Methods 5 through 8

are the closed-loop implementation of these methods. These methods are listed in Table II.

## IV. Comparison of Dynamically-Defined Virtual Fixture Methods

Two user experiments were performed to evaluate the virtual fixture methods. All methods were compared to the Static Wall Method in which the virtual fixture is located at the boundary of the forbidden region. In Experiment I, the users had no visual feedback of the task space and relied only on the haptic feedback from contact with the virtual fixture. Experiment II was conducted as a preliminary experiment in which visual feedback and cognitive load were provided to the user.

### A. Experimental Apparatus

Both experiments used the apparatus shown in Figure 4. The system includes a low-friction linear stage, an optical encoder, a non-backdrivable motor (1:128 gear ratio), a force sensor, and a tool attached rigidly to the force sensor. The force sensor used was the ATI Nano-17 (ATI Industrial Automation) which has a force sensing resolution of 0.0017N and sensing ranges of $\pm$37N along the $z$-axis, which was used to control the linear stage. Four elastic Nitinol strips connect the tool to the stage and simulate joint compliance. A spherical Delrin knob is used as the tool handle. A restraint with soft padding was used to minimize arm motion and keep the forearm parallel to the horizontal plane. Only the user's hand and wrist were allowed to move. A large blinder shown in Figure 4(a) was used to conceal the user's hand and stage. A camera is used to obtain the tool and stage position (Figure 4(b)) through real-time visual tracking. Kalman filter was used to integrate the measurements from the camera, encoder, and model to determine the stage and tool positions. The filter used the tracked stage and tool positions as the absolute measurements. The visual tracker provided the position update at 30Hz while the robot (encoder) updated at 500Hz. When the tracker information was not available, the filter used the velocity calculated from the encoder reading and the model to update the stage and tool positions.

### B. Experimental Method

In both experiments, the users were asked to move the stage at a moderate speed until contact is made with the virtual fixture at which point he/she would move the tool in the opposite direction until instructed to stop. The users were instructed to hold the tool with a comfortable grip and were asked to keep the grip posture consistent for each trial. We implemented the eight Dynamically-Defined Virtual Fixture methods shown in Table II and the Static Wall method. In Experiment I, twelve right-handed participants were involved in this experiment: 6 males and 6 females, ranging from the ages 18 to 29. The nine methods were applied in random order. Each user performed three trials of each method for a total of 27 trials.

As a preliminary study, only two users were included in Experiment II. Visual feedback was provided as a real-time display of the tool position and the forbidden-region boundary on the monitor. The display used a 1:1 scale in position. The cognitive load used in this experiment involved mental arithmetic, similar to [6] and [8]. During each trial, the experimenter called out a set of four random integers between 1 and 9 and two ordinal numbers between 1st and 4th which specified the numbers from the set that were to be added. The user was required to memorize the four integers, add the specified integers, and enunciate the answer. A total of four scenarios were tested: cognitive load only (CLO), no cognitive load and no visual feedback (NCV), cognitive load and visual feedback (CLVF), and visual feedback only (VFO). The NCV scenario is the one used in Experiment I. The user followed the same procedures of Experiment I except with the addition of three new scenarios, resulting in 108 trials total. Practice time was given in both experiments.

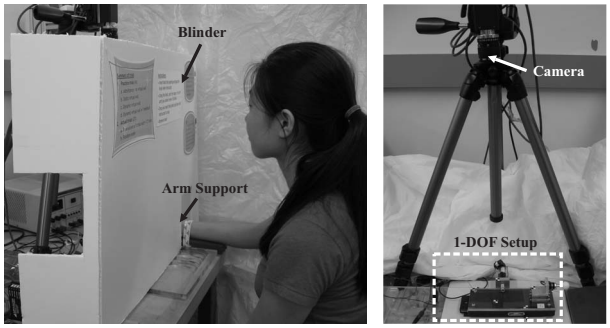


Fig. 4. The experimental setup showing in (a) a user with a blinder used to prevent a visual feedback of the stage and (b) the vision system used for a visual tracking of the stage and tool position. The 1-DOF setup is shown in detail in Figure 1(b).

To evaluate the methods, we applied an error metric called the *error ratio*. The error ratio is the distance between the maximum tool position and the forbidden-region boundary divided by the force applied when the maximum tool position was reached. Since the magnitude of the applied force, which directly affects the error, differs from trial to trial, the error ratio provides a more accurate comparison of the methods. Positive values of the ratio indicate penetration into the forbidden region. Therefore, a small negative error ratio is desirable since it indicates that the method is effective in preventing the tool from entering the forbidden region when a large force is applied. All methods are compared to the Static Wall case where the virtual fixture is placed at the forbidden-region boundary.

### C. Results of Experiment I: No Visual Feedback

We applied a mixed effects analysis of variance (ANOVA) to compare the error ratios obtained for each method. ANOVA showed a statistical difference in the mean error ratios with $P < 0.0001$ on a 95% confidence interval. The mean error ratios are shown in Figure 5. We observed penetration in the open-loop Velocity-Based Method (Method 1) and in the methods with the closed-loop controller (Methods 5-8). Subsequently, Scheffe's test was used for pairwise comparisons of the methods (Table III).

All users penetrated the forbidden region with the Static

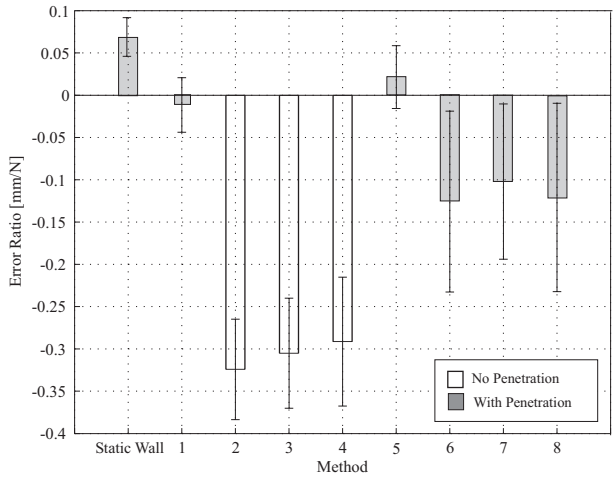


Fig. 5. Plots of the mean error ratio per method. Positive error ratios indicate penetration into the forbidden region. The grey bars indicate the methods for which penetration was observed.

Wall Method in all trials, as expected due to the hand dynamics and joint compliance. For the open-loop dynamic wall methods (Methods 1-4), users did not penetrate into the forbidden region except with the Velocity-Based Method (Method 1). The failure of this method can be expected and is attributed to the chosen time interval, $\Delta t$. Though the time interval was set according to human reaction time, the determination of the optimal time interval needs further analysis.

For the rest of the open-loop methods (Methods 2-4), there were no significant differences. In the Hand-Dynamic Method with hand damping (Method 4), the lowest damping value found in [11] was used to achieve a conservative estimate of overshoot across users. Hence, the effect of damping is minimal and the insignificant difference between Methods 3 and 4 is not surprising. There is also no statistical difference between the Force-Based Method and the Hand-Dynamic Methods. In both methods, the amount of overshoot is inversely proportional to the square root of the system stiffness and directly proportional to the square root of the system mass. It is also directly proportional to the applied force as shown in (4) and (8). The conservativeness of the methods depends on the relationship between these parameters.

In the Hand-Dynamic Methods, the maximum hand mass and the minimum hand stiffness found in [11] were used to give a conservative estimate of the maximum tool position for all users. The Force-Based Method includes the tool mass and joint compliance but not the hand mass and the hand stiffness in the model. With respect to the system stiffness, the Hand-Dynamic Methods will be less conservative because the overall stiffness of the system is increased. The hand stiffness value (460.72 N/m) is relatively small compared to the stiffness of the system (4347.83 N/m). By adding the hand mass, the total mass of the system nearly doubles, from 0.062 kg to 0.1211 kg. In this respect, the Hand-Dynamic Method would tend to be more conservative than the Force-Based Method. However, another contributing

TABLE III

PAIRWISE COMPARISONS OF THE MEAN ERROR RATIOS USING SCHEFFE'S METHOD

| 1 | 2 | 3 | 4 | 5 | 6 | 7 | 8 | Methods |
|---|---|---|---|---|---|---|---|---|
| • | • | • | • | • | • | • | • | Static Wall |
| | • | • | • | | • | • | • | 1 |
| | | | | • | • | • | • | 2 |
| | | | | • | • | • | • | 3 |
| | | | | • | • | • | • | 4 |
| | | | | | • | • | • | 5 |
| | | | | | | | | 6 |
| | | | | | | | | 7 |

• Significant difference in error ratio

factor, the applied force, was not regulated in each trial. Depending on the magnitude of the force, either method could be more or less conservative than the other. The unknown relationship of these parameters may contribute to the insignificant differences between the Hand-Dynamic and Force-Based methods shown in the experimental data. Even though significant differences were not seen between these methods, the Hand-Dynamic Methods may lead to significantly better performance than the Force-Based Method by adjusting the hand parameters according to user-specific models.

With the closed-loop control, we observed penetration in all methods (Methods 5-8). The pairwise comparisons show no statistically significant differences in error ratios between the closed-loop methods, except for the Velocity-Based Method. However, the occurrence of penetration was at least 50% higher in the Velocity-Based Method than the others. Similar error ratios are expected among all methods since the closed-loop controller should allow the tool to approach the forbidden region regardless of the method.

To investigate further why users penetrated into the forbidden region with the closed-loop methods, we examined plots of the force exerted and tool position versus time. We observed two characteristic force profiles. In the first profile (Figure 6(a)), there is a sudden change in the applied force after the closed-loop controller is activated. The abrupt force exertion is the user's response to the change in velocity which occurs when the closed-loop controller is activated. In this case, the high gear ratio of the motor prevents the stage from achieving the acceleration needed to counter the transient response resulting from the input force. This problem may be solved by using a high-powered motor. However, the acceleratory behavior with a high power source may not be desirable in a human-machine cooperative setting and in certain applications such as surgery.

In contrast, there is no significant change in force in the second profile (Figure 6(b)); a relatively constant force is applied before and after the activation of the closed-loop controller. We hypothesize that the overshoot in this case is due to the lack of haptic feedback upon contact with the virtual fixture and the friction in the gear. Users adapt to the gradual change in velocity commanded by the closed-loop controller, making them unaware of the virtual fixture. As the users continue to move toward the forbidden region, the close

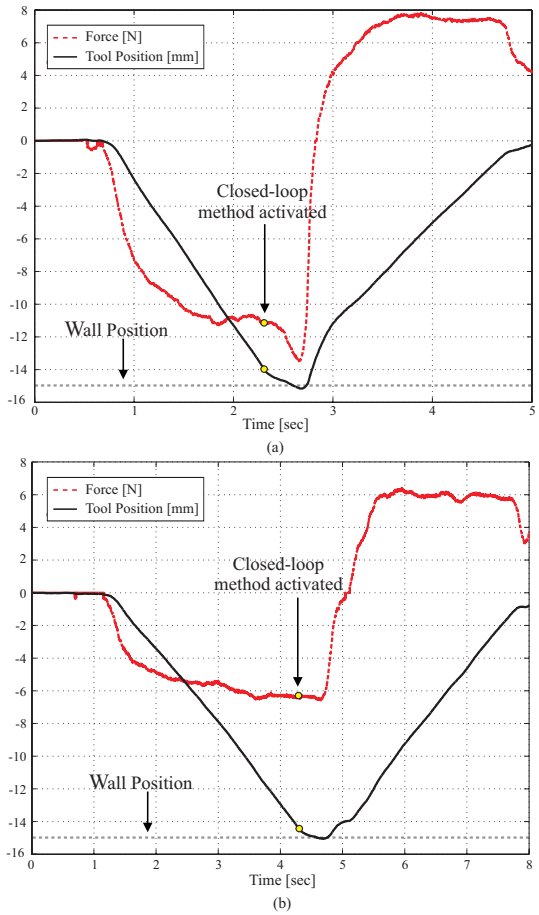


Fig. 6. Examples of two force profiles: (a) with abrupt force exertion and (b) with constant force, after the activation of the closed-loop controller.

proximity of the tool to the region causes the controller to output a small command velocity which translates to a small command motor torque. Until the position error results in a commanded torque large enough to overcome the friction in the gear and move the stage in the opposite direction, the tool continues to move past the boundary.

Similar trends were seen with the open-loop methods. The abrupt change in applied force is due to the complete stop of the stage upon virtual fixture contact. However, no penetration occurs in Methods 2-4 since the possible overshoot is accounted for when the dynamic virtual wall position was calculated. Since humans detect the change in velocity better than the change in position, we believe that a "crisp" haptic feedback such as the one observed in the open-loop methods provides crucial information for human-machine interaction with virtual fixtures.

### *D. Results of Experiment II: Visual Feedback and Cognitive Load*

From the results of Experiment I, the lack of haptic feedback is believed to contribute to the overshoot observed in the closed-loop methods. In an actual application of a human-machine interface, visual feedback of the task space is typically available. Hence, we conducted a preliminary experiment to investigate the effect of visual feedback on the performance of the Dynamically-Defined Virtual Fixture

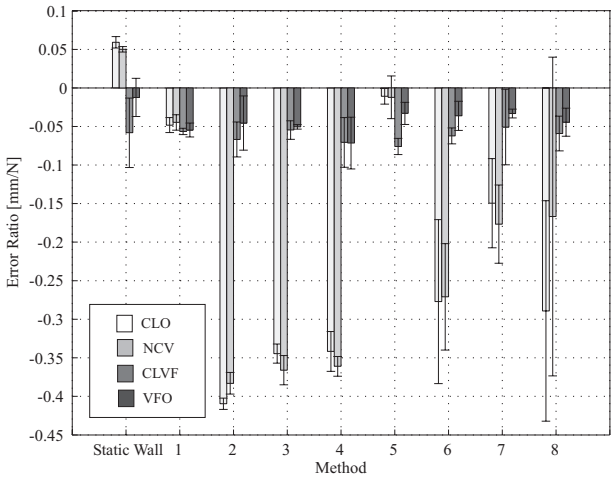


Fig. 7. Mean error ratios per method of one user performing Experiment II. CLO, NCV, CLVF, and VFO represent Cognitive Load Only, No Cognitive Load and No Visual Feedback, Cognitive Load and Visual Feedback, and Visual Feedback Only, respectively.

methods. In addition, cognitive load was introduced as a factor that could inhibit the user's ability to manipulate the robotic system. We hypothesize that the addition of visual feedback should result in less overshoot in all methods and decreased distance from the forbidden region in the closed-loop methods. We also predict that cognitive load should decrease the effectiveness of the methods.

As a preliminary assessment of our hypotheses, only two subjects participated in Experiment II. Due to the limited sample size, no statistical analysis was performed on the data collected. Based on the initial data, we did not observe a significant increase in error ratio as expected in the trials with the addition of cognitive load (Figure 7). This may be due to the simplicity of the pushing and pulling task. The addition of cognitive load may have a significant effect on a task with higher complexity and required skill level. However, a more extensive user experiment is required to validate the assumption. Figure 7 shows a significant difference with the addition of visual feedback. However, visual feedback alone does not prevent overshoot, as seen by cases of penetration with the Static Wall Method. The combination of visual feedback and dynamic virtual fixtures give the optimal condition. In all cases, we observe that visual feedback is a more influential factor than haptic feedback. Furthermore, the closed-loop methods benefit the most from visual feedback because the user has the ability to influence the tool position towards the forbidden region. However, addition of visual feedback will not benefit the open-loop methods, since the user needs to move against the virtual fixture in order to reach the forbidden-region boundary.

## V. Conclusions and Future Work

The No Visual Feedback experiment (Experiment I) showed the effectiveness of the open-loop Dynamically-Defined Virtual Fixture methods, namely the Hand-Dynamics and the Force-Based Methods, in preventing boundary penetration without statistical differences. The closed-loop controller decreased the distance from the forbidden region;

however, penetration was more prevalent. This was attributed to the lack of haptic feedback upon virtual fixture contact. Experiment II was conducted to evaluate the methods when visual feedback was used to compensate for the lack of haptic feedback. A cognitive load was added; however, no significant increase in boundary penetration was observed. In contrast, the initial results showed that the addition of visual feedback can lead to significant improvement in the performance of the closed-loop methods. This indicates the importance of both visual and haptic feedback in virtual fixture implementation.

In future work, the estimation of robot compliance and the user-specific hand parameters could be obtained in real-time using the vision system. User-specific implementation of the Hand-Dynamic Method should improve its performance over that of the Force-Based Method. The implementation of Dynamically-Defined Virtual Fixtures needs to be extended for systems with higher degrees of freedom. In addition, the effect of visual feedback and cognitive load on virtual fixture performance (and vice versa) pose interesting questions for further investigation.

## VI. Acknowledgements

The authors gratefully acknowledge Ankur Kapoor for his valuable suggestions on the project and Dr. Darius Burschka for his help with the vision system.

## References

[1] J. J. Abbott, P. Marayong, and A. M. Okamura. Haptic virtual fixtures for robot-assisted manipulation. *International Symposium of Robotics Research*, 2005.

[2] A. Bettini, P. Marayong, S. Lang, A. M. Okamura, and G. D. Hager. Vision assited control for manipulation using virtual fixtures. *IEEE Transactions Robotics and Automation*, 20(6):953–966, 2004.

[3] E. Bizzi, N. Hogan, F. A. Mussa-Ivaldi, and S. Giszter. Does the nervous system use equilibrium-point control to guide single and multiple joint movements. *Journal of Behavioral and Brain Sciences*, 15:603–613, 1992.

[4] K. R. Boff and J. E. Lincoln. *Engineering data compendium: Human perception and performance*, volume 3. Wright-Patterson Air Force Base, Ohio, 1988.

[5] A. Z. Hajian and R. D. Howe. Identification of the mechanical impedance at the human finger tip. *Journal of Biomechanical Engineering*, 119:109–114, 1997.

[6] K. Kobayashi and S. Yamada. Human-robot interaction design for low cognitive load in cooperative work. *13th International Workshop on Robot and Human Interactive Communication*, pages 569–574, 2004.

[7] K. J. Kuchenbecker, J. G. Park, and G. Niemeyer. Characterizing the human wrist for improved haptic interaction. *International Mechanical Engineering Congress and Exposition*, 72(1):591–598, 2003.

[8] D. Lamble, T. Kauranen, M. Laakso, and H. Summala. Cognitive load and detection thresholds in car following situations: safety implications for using mobile (cellular) telephones while driving. *Accident Analysis and Prevention*, 31:617–623, 1999.

[9] M. Li. *Intelligent robotic surgical assistance for sinus surgery*. PhD thesis, Johns Hopkins University, 2005.

[10] M. Li and R. H. Taylor. Spatial motion constraints in medical robot using virtual fixtures generated by anatomy. *IEEE International Conference on Robotics and Automation*, pages 1270–1275, 2004.

[11] P. Marayong, G. D. Hager, and A. M. Okamura. Effect of hand dynamics on virtual fixtures for compliant human-machine interfaces. *Symposium on Haptic Interfaces for Virtual Environments and Teleoperator Systems*, pages 109–115, 2006.

[12] C. A. Moore, M. A. Peshkin, and J. E. Colgate. Cobot implementation of virtual paths and 3-d virtual surfaces. *IEEE Transactions Robotics and Automation*, 19(2):347–351, 2003.

[13] S. Payandeh and Z. Stanisic. On application of virtual fixtures as an aid for telemanipulation and training. *Symposium on Haptic Interfaces for Virtual Environments and Teleoperator Systems*, pages 18–23, 2002.

[14] L. Rosenberg. Virtual fixtures: Perceptual tools for telerobotic manipulation. *Proceedings of IEEE Virtual Reality International Symposium*, pages 76–82, 1993.

[15] R. Taylor, A. Barnes, R. Kumar, P. Gupta, Z. Wang, L. Whitcomb P. Jensen, E. de Juan, D. Stoianovici, and L. Kavoussi. Steady-hand robotic system for microsurgical augmentation. *International Journal of Robotics Research*, 18(12):1201–1210, 1998.

[16] T. Tsuji, K. Goto, M. Moritani, M. Kaneko, and P. Morasso. Spatial chracteristics of human hand impedance in multi-joint arm movements. *IEEE/RSJ International Conference on Intelligent Robots and Systems*, 1:423–430, 1994.